Effect of SDF-1/CXCR4 axis on the migration of transplanted bone mesenchymal stem cells mobilized by erythropoietin toward lesion sites following spinal cord injury

JUN LI[1*], WEICHUN GUO[1*], MIN XIONG[2], HENG HAN[2], JIE CHEN[2], DAN MAO[2], BING TANG[2], HUALONG YU[2] and YUN ZENG[2]

[1]Department of Orthopaedics, Renmin Hospital of Wuhan University, Wuhan, Hubei 430060; [2]Department of Orthopaedics, Dongfeng General Hospital, Hubei University of Medicine, Shiyan, Hubei 442008, P.R. China

Received February 23, 2015; Accepted July 15, 2015

DOI: 10.3892/ijmm.2015.2344

Abstract. Accumulating evidence has indicated that the stromal cell-derived factor-1 (SDF-1)/CXC chemokine receptor 4 (CXCR4) axis plays a crucial role in the recruitment of bone marrow-derived mesenchymal stem cells (BMSCs) into lesion sites in animal models. The aim of this study was to investigate the effects of the SDF-1/CXCR4 axis on the migration of transplanted BMSCs mobilized by erythropoietin (EPO) toward the lesion site following spinal cord injury (SCI). A model of SCI was established in rats using the modified Allen's test. In the EPO group, EPO was administered at a distance of 2 mm cranially and then 2 mm caudally from the site of injury. In the BMSC group, 10 μl of BMSC suspension was administered in the same manner. In the BMSC + EPO group, both BMSCs and EPO were administered as described above. In the BMSC + EPO + AMD3100 group, in addition to the injection of BMSCs and EPO, AMD3100 (a chemokine receptor antagonist) was administered. The Basso-Beattie-Bresnahan (BBB) Locomotor Rating Scale and a grid walk test were used to estimate the neurological recovery following SCI. Enzyme-linked immunosorbent assay (ELISA) was performed to assess the tumor necrosis factor-α (TNF-α) and SDF-1 expression levels. An immunofluorescence assay was performed to identify the distribution of the BMSCs in the injured spinal cord. A Transwell migration assay was performed to examine BMSC migration. A terminal deoxynucleotidyl transferase-mediated dUTP nick-end labeling (TUNEL) assay was performed to detect the apoptotic index (AI). Western blot analysis was performed to measure the expression levels of erythropoietin receptor (EPOR) and CXCR4. Significant improvements in locomotor function were detected in the BMSC + EPO group compared with the BMSC group ($P<0.05$). GFP-labeled BMSCs were observed and were located at the lesion sites. Additionally, EPO significantly decreased the TNF-α levels and increased the SDF-1 levels in the injured spinal cord ($P<0.05$).The AI in the BMSC + EPO group was significantly lower compared with that in the other groups ($P<0.05$). Furthermore, EPO significantly upregulated the protein expression of CXCR4 in the BMSCs and promoted the migration of the BMSCs, whereas these effects were markedly inhibited when the BMSCs were co-transplanted with AMD3100. The findings of the present study confirm that EPO mobilizes BMSCs to the lesion site following SCI and enhances the anti-apoptotic effects of the BMSCs by upregulating the expression of SDF-1/CXCR4 axis.

Introduction

Spinal cord injury (SCI), which results from primary and secondary injury mechanisms (1), is the most devastating complication of spinal trauma, often resulting in progressive sensory and functional damage. In addition to the severe physical and psychological harm experienced by patients themselves, SCI also imposes a huge economic burden on society (2). Despite years of research and numerous attempts at various treatment strategies, the remedy for paralysis remains elusive and current treatments are restricted to the early administration of large doses of methylprednisolone and immediate surgical intervention to alleviate spinal cord edema (3,4). Recent advances in SCI research have drawn attention to an array of novel experimental therapeutic approaches (5).

Of all the potential strategies, bone marrow-derived mesenchymal stem cells (BMSCs) appear to be a most promising candidate for clinical application, since they have been demonstrated to be helpful in the repair of injured spinal cords in experimental animals (6-8). The administration of BMSCs, with minimal delay, has been suggested as a way of attenuating secondary injury and maximizing the volume of spared neuro-

Correspondence to: Dr Min Xiong, Department of Orthopedics, Dongfeng General Hospital, Hubei University of Medicine, 18 Daling Road, Shiyan, Hubei 442008, P.R. China
E-mail: mrorthopedics@sina.com

*Contributed equally

Key words: stromal cell-derived factor-1/CXC chemokine receptor 4 axis, bone marrow-derived mesenchymal stem cells, erythropoietin, spinal cord injury

logical tissue (9). However, the homing process of BMSCs is inefficient due to cell apoptosis, as well as limitations in the cellular signals that modulate their recruitment (10,11). It has been shown that the majority of transplanted BMSCs are unable to reach the lesion site, and this results in a limited therapeutic effect (12,13). Accumulating evidence has indicated that the stromal cell-derived factor-1 (SDF-1)/CXC chemokine receptor 4 (CXCR4) axis plays a crucial role in the recruitment of BMSCs to lesion sites in animal models (14-17). It has been demonstrated that *in vitro*-amplified BMSCs display a downregulation in the surface expression of cardinal homing receptors, compromising CXCR4 and their capacity to react to homing signals (18,19). Thus, an alternative strategy has to be explored to enhance the therapeutic benefits of BMSCs.

Erythropoietin (EPO) is a glycoprotein that mediates the differentiation and apoptosis of a number of non-hematopoietic cells via the erythropoietin receptor (EPOR) (20). There is increasing evidence for the different roles of EPO in various types of diseases, such as calvarial defects (21), chronic renal failure (22) myocardial infarction (23), osteonecrosis of the femoral head (24), spinal cord injury (25,26), diabetes mellitus (27) and acute lung injury (28,29). The study by Zwezdaryk *et al* (30) confirmed that EPOR is also expressed on the surface of BMSCs. The study by Liu *et al* (31) demonstrated that EPO promotes the proliferative effects of BMSCs in an acute kidney injury microenvironment and reverses their low secretory capacity. Nair *et al* (32) demonstrated the tremendous potential of EPO to mobilize BMSCs to migrate to the defective bone tissue and to promote the osteogenic differentiation of BMSCs.

On the basis of the above-mentioned findings, we hypothesized that EPO may mobilize the BMSCs to migrate to the lesion site following SCI and promote recovery; we hypothesized that the SDF-1/CXCR4 axis plays an important role in this process. Thus, in this study, we aimed to confirm this hypothesis and elucidate the possible molecular mechanisms involved, in order to provide new ideas for research into clinical treatments for SCI.

Materials and methods

Animals. The present study was conducted using adult female Sprague-Dawley (SD) rats (n=108; weighing 200-250 g). All rats used in this study were purchased from the Animal Experiment Center of Hubei University of Medicine (Wuhan, China). The study protocol was approved by the Ethics Committee on Animal Experiments of Hubei University of Medicine (Shiyan, China; protocol no. SYXK20 110008). The rats were housed 3 per cage for approximately 1 week prior to the start of the experiments, with free access to food and water and maintained in a suitable environment at 21˚C, 60% air humidity and a 12-h light/dark cycle.

Creation of rat model of acute SCI. Following a baseline behavioral assessment, a model of SCI was established in rats using the modified Allen's test, as previously described (33). The rats were anesthetized with an intraperitoneal injection of 10% chloral hydrate (0.3 ml/100 g) following 12 h of pre-operative fasting from food and water. Under sterile conditions, a dorsal laminectomy was performed, centering on the T9 spinous process, and the spinal cord was then exposed. Subsequently, each rat sustained a contusive SCI from a Spinal Cord Impactor (W.M. Keck Center for Collaborative Neuroscience, Rutgers, Piscataway, NJ, USA), with a 10 g impact rod vertically dropped from a height of 5 cm which then impinged on the spinal cord in a circular zone with a 2 mm diameter. The dwell time for each injury was 10 sec which was sufficient to cause a moderate contusion. The release weight, height of drop, and velocity of each SCI were determined using the Spinal Cord Impactor software (version 7.5). The signs of the successful infliction of SCI were as follows: the rat tails swung spastically, there was a retraction of the lower limbs and a torso-like flutter, and both lower extremities exhibited flaccid paralysis. In the sham-operated group, the spinal cord was exposed in the same manner, but without subjecting the rats to a contusive SCI.

Derivation and culture of BMSCs. The BMSCs were isolated as previously described (34). Briefly, another 10 SD rats (weighing 120±20 g) were sacrificed following anesthesia with an intraperitoneal injection of 10% chloral hydrate (0.3 ml/100 g). Under aseptic conditions, the BMSCs were separated from the tibias and femurs and all conterminal tissues were carefully removed. The extracted BMSCs were centrifuged at 1,000 x g for 5 min and then aseptically plated in Dulbecco's modified Eagle's medium (DMEM; HyClone, Logan, UT, USA) supplemented with 10% fetal bovine serum (FBS; Invitrogen, Carlsbad, CA, USA), 2 ml glutamine and 100 U/ml penicillin. The cells were incubated at 37˚C, in 5% CO_2 for 24 h and the culture medium was then replaced. This procedure was performed every 72 h, through which the other non-adherent cells were eliminated. The remaining BMSCs were examined everyday with an inverted phase contrast microscope (Eclipse Ti-E/U/S; Nikon, Tokyo, Japan) to verify that the cells were further amplified. The BMSCs were subcultured at 1:3 every 4 days when they reached approximately 80-90% confluence. Those used for transplantation were subjected to trypsin preconditioning and washed with phosphate-buffered saline (PBS). To trace the internal migration of the BMSCs toward the lesion site following SCI, transfection was carried out using a recombinant adenovirus encoding green fluorescent protein (Ad-GFP) plasmid with Lipofectamine 2000 (Cyagen Biosciences Inc., Santa Clara, CA, USA), in accordance with the manufacturer's instructions. At 6 h after transfection, the medium was exchanged with all nutrition culture medium and transgene expression was examined 2 days later using a fluorescence microscope (Eclipse Ti-E/U/S; Nikon).

Experimental groups and treatments. A total of 108 rats were randomly divided into 6 groups (n=18/group) as follows: i) the sham-operated group; ii) the model control group; iii) the EPO group; iv) the BMSC group; v) the BMSC + EPO group; and vi) the BMSC + EPO + AMD3100 group. Each animal in the experimental groups was subjected to SCI as described above. In the EPO group, recombinant human EPO (rhEPO; Beijing Four Rings Bio-Pharmaceutical Co., Ltd., Beijing, China) was administered at a distance of 2 mm cranially and then 2 mm caudally from the site of injury ($5x10^3$ IU/kg) using a prefilled syringe. In the BMSC group, 10 μl of BMSC suspension containing approximately $3x10^4$ cells was administered via a microsyringe (Hamilton, Reno, NV, USA). In the BMSC + EPO group, BMSCs and EPO were administered as

described above. In the BMSC + EPO + AMD3100 group, in addition to the injection of BMSCs and EPO, AMD3100 (a chemokine receptor antagonist; Pfizer, Inc., New York, NY, USA) was administered in the same manner (5 mg/kg) through a microsyringe (Hamilton). The AMD3100 dosage was selected in accordance with a previous study (35). In the model control and sham-operated groups, 10 μl of PBS was injected. Following withdrawal of the microsyringe, the muscles and the skin were stitched in respective layers.

Post-operative care. All the rats were administered penicillin ($3x10^4$ U/kg) and an analgesic, sufentanil (0.05 μg/kg), for the first 3 days. The urinary bladders were manually emptied by squeezing twice a day until the auto-urination function was restored. Food and water were supplied in slender drinking tubes by placing them at the bottom of the cage, until the rats were able to lift their heads to reach the food placed at a normal height/position in the cage. Rats diagnosed with bacterial infections during the experiment were treated immediately with cefazolin (10 mg/kg/day; Sandoz International GmbH, Holzkirchen, Germany).

Neurological evaluation. Dual hind limb motor function was evaluated at 1, 3, 7, 14, 21 and 28 days post-SCI using the Basso-Beattie-Bresnahan (BBB) Locomotor Rating Scale developed by Basso *et al* (36). A 120x30 cm foam box with a smooth bottom was manufactured for the assessment. The rats were placed in the box 2 days pre-operatively, twice a day in order to familiarize them with the environment. The dual hind limb motor function was quantified using a scale ranging from 0 to 21, where 0 corresponds to no locomotor activity and 21 corresponds to normal performance. A sensorimotor grid walk test was also conducted to estimate the capacity of the rats to precisely control hind paw placement, as previously described (37). The rats crawled freely on a 120x120 cm grid with 1.0 cm regularly spaced horizontal holes. Slips were recorded when the animal misplaced the paw down through the hole in the grid, until a maximum value of 20 missteps were reached. The rats that could not perform with at least proficient gait in the BBB test were unable to finish the walkway and were classified according to the maximum value. To decrease the average error and improve the accuracy, all evaluations were performed using a double blind technique: two individuals observed from different sides and recorded the scores independently, and the mean values were then acquired.

Enzyme-linked immunosorbent assay (ELISA). Thoracic spinal cord segments (approximately 1-cm-thick) centered on the site of injury were serially collected and then immediately homogenized at 1, 7 and 28 days post-operation. The samples were centrifuged at 1,800 x g at 4˚C for 10 min, and subsequently, the detached spinal cord samples were stored at -80˚C for further research. The levels of cytokines, including tumor necrosis factor-α (TNF-α) and SDF-1 levels were measured using DuoSet ELISA kits (Elabscience Biotechnology Co., Ltd., Shanghai, China) in accordance with the manufacturer's instructions. All analyses were carried out in duplicate, using the proposed substrates, buffers and diluents. Each experiment was repeated 4 times. The final outcomes were pooled as the average concentration of cytokines.

Immunofluorescence assay. To identify the distribution of the BMSCs in the injured spinal cord, an immunofluorescence assay was performed 2 weeks following surgery. On days 1, 7 and 28 following treatment, 6 animals from each group were randomly selected and were sacrificed by anesthesia. The injured spinal cord tissues were carefully extracted. At each time point, 4 specimens from each group were fixed with 4% paraformaldehyde for 24 h and then stored at -80˚C in a constant temperature refrigerator for biological detection. Two specimens were frozen and embedded in OCT (Leica Biosystems, Shanghai, China), and then cut into 7-μm-thick longitudinal cryostat sections. To reduce non-specific staining, the sections were treated with diluted normal goat serum (Boster Bio-Engineering, Wuhan, China) at room temperature for 30 min. To stain the nuclei, 4',6-diamidino-2-phenylindole (DAPI) was added and followed by incubation in the dark for 5 min. The excess DAPI was washed 4 times for 5 min with Tween-20 in PBS (PBST; Beyotime Institue of Biotechnology, Beijing, China) following incubation. The slices were then dried with absorbent paper and mounted with anti-fluorescent quencher (SouthernBiotech, Wuhan, China). Immunofluorescence was observed under a fluorescence microscope (Olympus BX51; Olympus, Tokyo, Japan).

Transwell migration assay. Cellular migration was detected using Transwell chambers, which were 6.5 mm in diameter with 8 μm nitrocellulose pore filters (Amersham Biosciences, Piscataway, NJ, USA). In the chemotaxis group, 200 μl of serum-free culture medium containing $1x10^5$ BMSCs were added to the upper chambers, and 800 μl of DMEM containing 10 U/ml of rhEPO (Beijing Four Rings Bio-Pharmaceutical Co., Ltd.) and 10% FBS were added to the lower chambers. In the chemotaxis inhibition group, 200 μl of serum-free culture medium containing $1x10^5$ BMSCs, which had been co-cultured with 10 μg/ml AMD3100 (Pfizer Compounds) at 37˚C for 2 h, were added to the upper chambers, and 800 μl of DMEM containing 10 U/ml of rhEPO and 10% FBS were added to the lower chambers. In the control group, 200 μl of serum-free culture medium containing $1x10^5$ BMSCs were added to the upper chambers, and 800 μl of DMEM were added to the lower chambers. Following incubation for 18 h, the non-migrated cells in the upper chamber were cleared and the membranes were fixed with 4% paraformaldehyde for 30 min. The migrated cells were stained with 5% crystal violet dye solution (Saichuang Technology, Wuhan, China) for 20 min, washed with PBS, and then photographed under a microscope (Eclipse Ti-E/U/S; Nikon).

Terminal deoxynucleotidyl transferase-mediated dUTP nick-end labeling (TUNEL) assay. The apoptotic index (AI) of the lesion area was detected by TUNEL assay using an *In Situ* Cell Death Detection kit (Roche Applied Science, Basel, Switzerland) according to the manufacturer's instructions. The sections were dewaxed with graded alcohols and then digested with protease K (20 μg/ml, pH 7.4) at 25˚C for 30 min. The sections were then incubated with TUNEL reaction mixture, which contained 5 μl of enzyme solution and 45 μl of fluorochrome-labeled solution at 37˚C without light for 60 min. After being washed with PBS 3 times, the sections were incubated with DAPI (Beyotime Institue of Biotechnology) for 30 min. Subsequently, the sections were dried with absorbent paper and mounted with anti-fluorescent quencher liquid (Southern

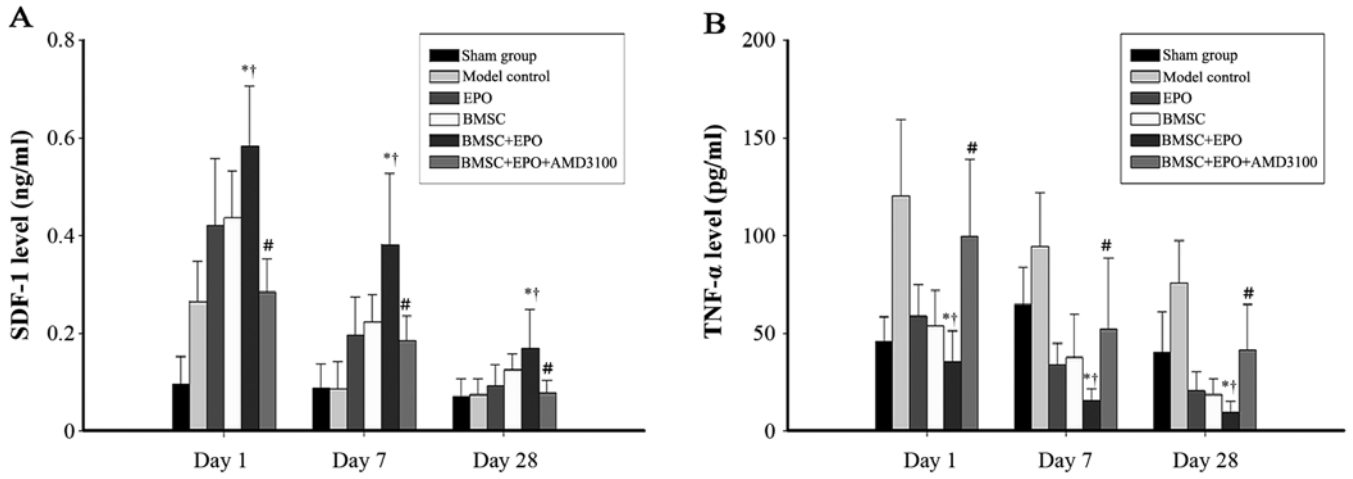

Figure 1. Detection of SDF-1 and TNF-α levels in the rat spinal cords on days 1, 7 and 28 post-operation in each group. (A) SDF-1 levels. *P<0.05 vs. the sham-operated (sham) group and model control group; †P<0.05 vs. the EPO, BMSC and BMSC + EPO + AMD3100 groups; #P>0.05 vs. the model control group. (B) TNF-α levels. *P<0.05 vs. the sham group and model control group; †P<0.05 vs. the EPO, BMSC and BMSC + EPO + AMD3100 groups; #P>0.05 vs. the model control group. The data are plotted as the means ± SD. SDF-1, stromal cell-derived factor-1; TNF-α, tumor necrosis factor-α; EPO, erythropoietin; BMSC, bone marrow-derived mesenchymal stem cell.

Biotech, Birmingham, AL, USA) and then observed under a fluorescence microscope (Eclipse Ti-E/U/S; Nikon). Apoptotic nuclei with green fluorescence and DAPI-positive nuclei with blue fluorescence were observed at x400 magnification. The AI was calculated as the percentage of TUNEL-positive cells among the total number of nucleated cells.

Western blot analysis. The spinal cord samples were homogenized using radioimmunoprecipitation lysis buffer (RIPA; Beyotime Institue of Biotechnology) and then centrifuged at 18,000 x g for 15 min. The supernatant containing 50 μg total protein was extracted for electrophoresis on a 10% sodium dodecyl sulfate gel (SDS; Beyotime Institute of Biotechnology) and then transferred onto polyvinylidene fluoride membranes (PVDF; Millipore, Billerica, MA, USA). After being blocked with Tris-buffered saline with Tween-20 (TBST; Biosciences, Shanghai, China), the PVDF membranes were incubated at 4˚C overnight with anti-CXCR4 (P61073) or anti-EPO antibody (sc-80995; 1:200; Santa Cruz Biotechnology, Inc., Santa Cruz, CA, USA) or rabbit anti-GAPDH antibody (A300-639A; 1:200; Xianzhi Biological Co. Ltd., Hangzhou, China) as primary antibodies, followed by incubation with horseradish peroxidase-labeled goat anti-rabbit secondary antibody (A00098; 1:50,000; Santa Cruz Biotechnology, Inc.) at 26˚C for 2 h. The immunoreactive complexes were visualized using an ECL enhanced detection kit (Thermo Fisher Scientific, Waltham, MA, USA) and exposed to X-ray films. The densitometry of the bands was analyzed using Image-Pro Plus 6.0 software (Media Cybernetics, Rockville, MD, USA). The expression of CXCR4 and EPO was then normalized to GAPDH.

Statistical analysis. All data are expressed as the means ± standard deviation (SD) and compared by one way analysis of variance (ANOVA). All statistical analyses were conducted using Statistical Product and Service Solutions (SPSS) version 19.0 software (IBM Corp., Armonk, NY, USA), with a value of P<0.05 considered to indicate a statistically significant difference.

Results

TNF-α and SDF-1 levels in rat spinal cords. The levels of SDF-1 in the spinal cord increased significantly following SCI (Fig. 1A). The SDF-1 levels in the BMSC + EPO group were significantly higher compared with those in the sham-operated, model control, EPO, BMSC and BMSC + EPO + AMD3100 groups (P<0.05). However, no significant difference was observed between the model control and BMSC + EPO + AMD3100 groups. On days 1, 7 and 28 post-SCI, the TNF-α levels (Fig. 1B) in the BMSC + EPO group were significantly lower than those in the sham-operated, model control, EPO, BMSC and the BMSC + EPO + AMD3100 groups (P<0.05). However, the difference was not significant between the model control and BMSC + EPO + AMD3100 groups (P>0.05).

The administration of BMSCs together with EPO improves neurological recovery following SCI. Dual hind limb locomotor function was evaluated using two complementary behavioural tests. The BBB motor rating scale was adopted to evaluate the locomotor capacity of the animals in each group up to 28 days post-operation (Fig. 2). Due to the effect of the anesthesia, no significant difference was observed between the rats subjected to SCI on day 1 post-operation. The mean BBB scores in the sham-operated group declined slightly at the beginning, but returned to normal values by day 7. Over time, the rats in the BMSC + EPO group obtained significantly higher BBB scores than those of the rats in the model control and BMSC + EPO + AMD3100 group (P<0.001) and those of the rats in the EPO and BMSC group (P<0.05). However, no significant differences were observed between the model control and BMSC + EPO + AMD3100 groups (P>0.05). The grid walk test of the hind limbs was applied to estimate locomotor coordination and motor accuracy (Fig. 3). The animals administered the BMSCs in conjunction with EPO exhibited progressive improvement in hind limb control and

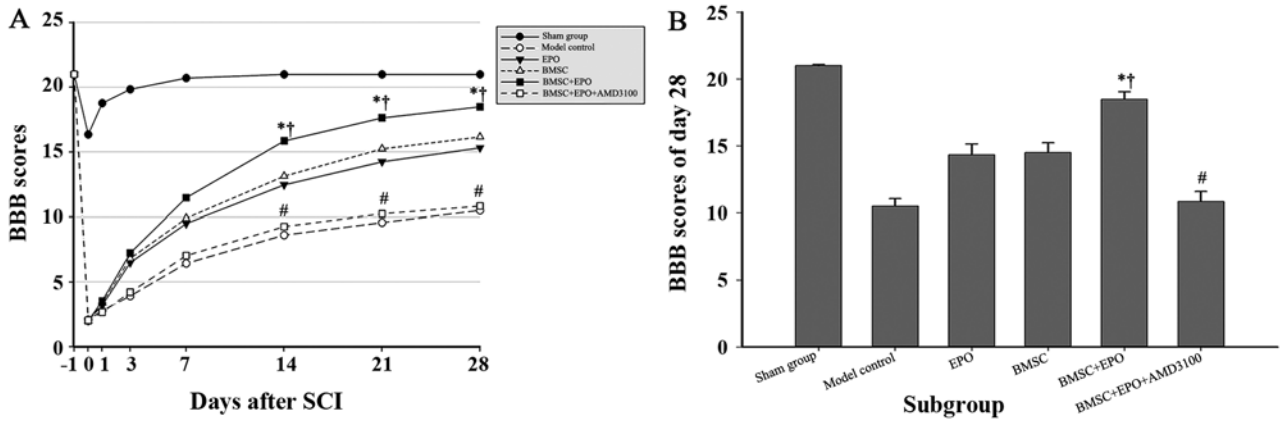

Figure 2. (A) Time course of functional recovery of hind limbs post-operation in each group. (B) Bar graph representing the assessment of motor function recovery by BBB scores on day 28 post-operation. *P<0.001 vs. the BMSC + EPO + AMD3100 and model control groups; †P<0.05 vs. the EPO and BMSC groups; #P>0.05 vs. the model control group. The data are plotted as the means ± SD. BBB, Basso-Beattie-Bresnahan; EPO, erythropoietin; BMSC, bone marrow-derived mesenchymal stem cell.

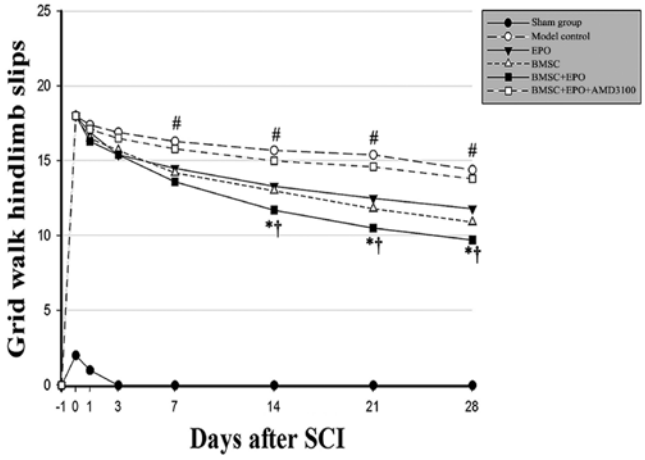

Figure 3. Time course of grid walk test of hind limbs post-operation in each group. *P<0.001 vs. the BMSC + EPO + AMD3100 and model control groups; †P<0.05 vs. the EPO and BMSC groups; #P>0.05 vs. the model control group. The data are plotted as the means ± SD. EPO, erythropoietin; BMSC, bone marrow-derived mesenchymal stem cell. Sham group, sham-operated group.

paw placement accuracy in the grid walk test. Moreover, the BMSC + EPO-treated rats experienced significantly fewer hind limb slips from day 7 than the rats in the model control and BMSC + EPO + AMD3100 groups (P<0.001) and the rats in the EPO and BMSC group (P<0.05); however, no significant differences were observed in these scores between the model control and the BMSC + EPO + AMD3100 groups (P>0.05).

Detection of fluorescently-labeled cells in injured spinal cords. The transplanted cells were detected in the injured spinal cords 2 weeks following SCI (Fig. 4). GFP-labeled BMSCs were observed and they were located at the lesion site in the BMSC and BMSC + EPO groups. However, homologous cells were almost undetectable in the sham-operated, model control, EPO and BMSC + EPO + AMD3100 groups.

EPO induces BMSC migration in vitro. Our results (Fig. 5) revealed that EPO significantly promoted the migration of BMSCs when compared with the control group (no EPO; P<0.001); however, the EPO-induced cell migration was markedly inhibited when the BMSCs were preconditioned with AMD3100 (P<0.001). No significant differences were observed between the AMD3100 group and the control group (P>0.05).

EPO reduces the AI in the lesion site following SCI. The AIs at different time points following SCI in each group are presented in Figs. 6 and 7. The quantity of TUNEL-positive cells on day 1 following SCI showed no significant difference between the model control, EPO, BMSC, BMSC + EPO and BMSC + EPO + AMD3100 groups. On days 7 and 28 post-SCI, the AI in the BMSC group was significantly lower than that in the model control group (P<0.05) and the AI in the BMSC + EPO group was significantly lower than that in the model control, EPO, BMSC and BMSC + EPO + AMD3100 groups (P<0.05); however, the difference between the model control and BMSC + EPO + AMD3100 groups was not statistically significant (P>0.05). These data indicated that EPO enhanced the anti-apoptotic effect of the BMSCs, which was attenuated by AMD3100.

EPO enhances the protein expression of CXCR4 in BMSCs. The protein expression levels of EPOR and CXCR4 were measured by western blot analysis (Fig. 8). The protein expression of EPOR increased with the administration of EPO and then gradually decreased from day 7 to 28 (Fig. 8A). No significant differences were observed in EPOR protein expression between the sham-operated, model control and BMSC groups. The CXCR4 expression level in the EPO and BMSC + EPO groups was consistent with the expression data obtaeind for EPOR; however, this effect was antagonized with the administration of AMD3100 (Fig. 8B).

Discussion

With the development of transplantation and regenerative medicine, an array of novel strategies have been proposed to facilitate functional recovery following SCI. These efforts have been principally focused on the attenuation of the

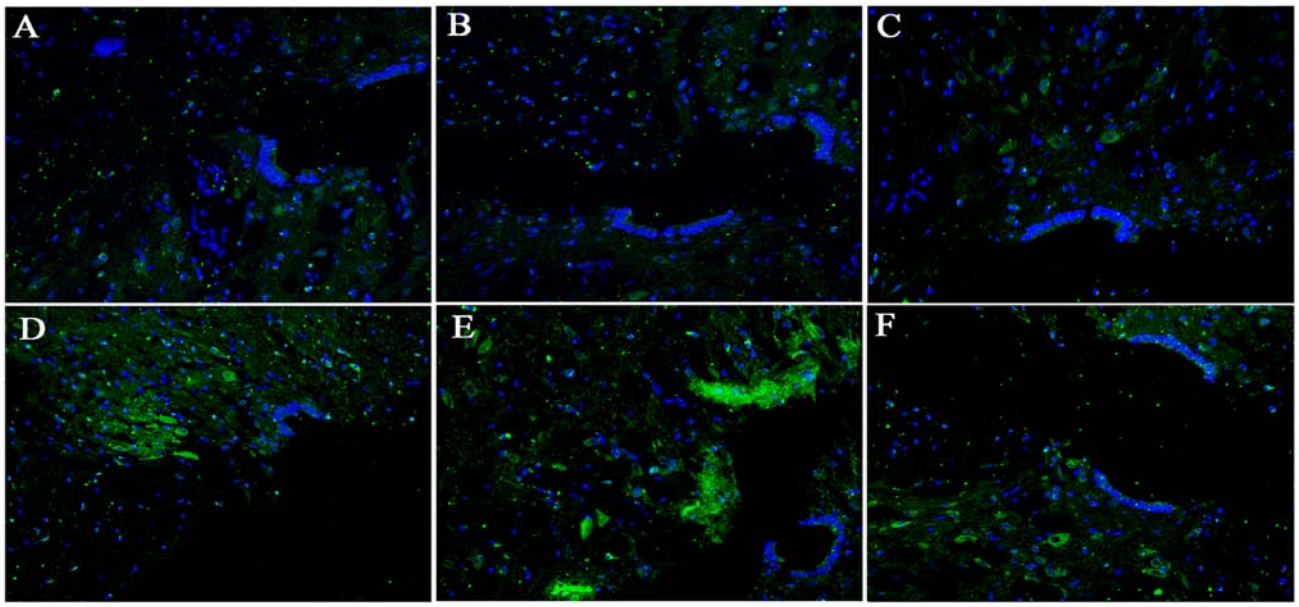

Figure 4. Localization of fluorescently-labeled cells transplanted into the injured spinal cord. (A) The sham-operated group, (B) model control, (C) EPO, (D) BMSC, (E) BMSC + EPO, and (F) BMSC + EPO + AMD3100 groups. GFP fluorescently-labeled BMSCs (green) and DAPI positive nuclei (blue) were observed at the lesion site following SCI. Bar, 400 μm. EPO, erythropoietin; BMSC, bone marrow-derived mesenchymal stem cell; GFP, green fluorescent protein; SCI, spinal cord injury.

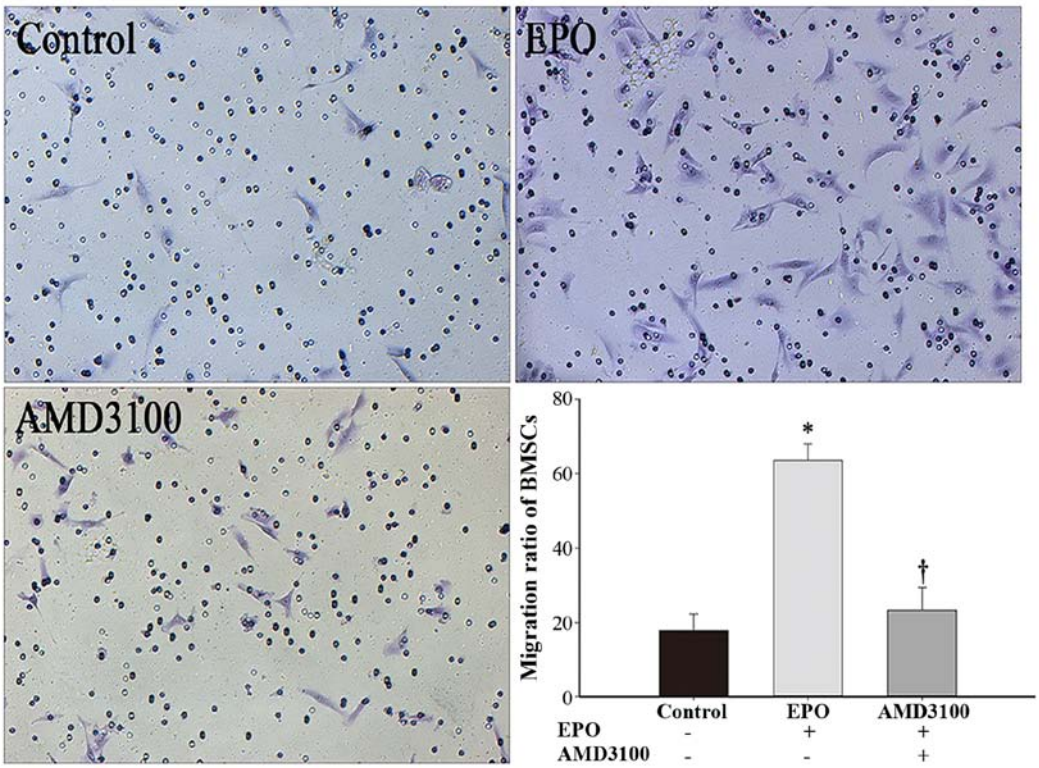

Figure 5. Enhanced BMSC recruitment around EPO-loaded implants. *P<0.001 vs. the control and AMD3100 groups; †P>0.05 vs. the control group. The data are plotted as the means ± SD. EPO, erythropoietin; BMSC, bone marrow-derived mesenchymal stem cell.

secondary delayed damage cascade that compounds a series of pathophysiological courses which hinder repair following autologous transplantation and remyelination (4,38). The potential application of BMSCs in the treatment of SCI is being widely investigated, yet it appears that this strategy alone is inefficient, while a combined strategy seems to be more promising. EPO, also known as red blood cell growth factor, is a glycoprotein containing sialic acid with a molecular weight of 34 kDa. EPO exerts its physiological effects by binding to its specific cell surface receptor, EPOR (39). The reason that

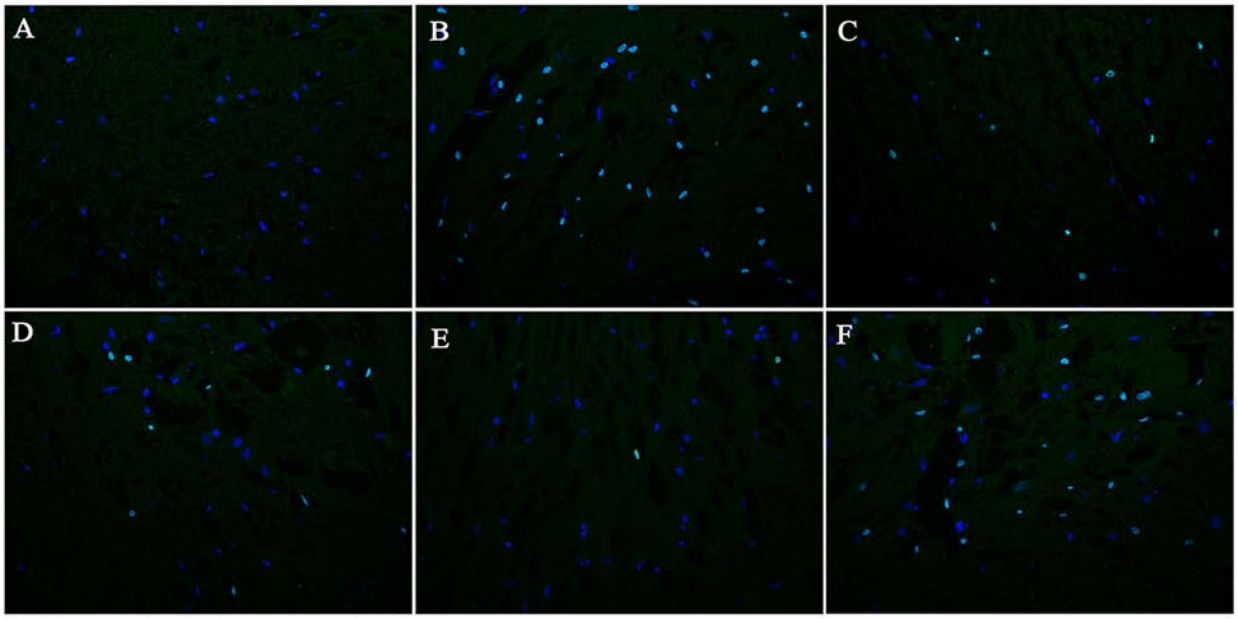

Figure 6. Apoptosis in the injured spinal cords on day 7 following SCI (magnification, x400). (A) The sham-operated group, (B) model control, (C) EPO, (D) BMSC, (E) BMSC + EPO, (F) BMSC + EPO + AMD3100 groups. The TUNEL-positive nuclei showed green fluorescence and DAPI-positive nuclei showed blue fluorescence. The number of TUNEL-positive cells was significantly lower in the BMSC + EPO group compared with the model control, EPO, BMSC, BMSC + EPO and BMSC + EPO + AMD3100 groups. Bar, 400 μm. EPO, erythropoietin; BMSC, bone marrow-derived mesenchymal stem cell; SCI, spinal cord injury.

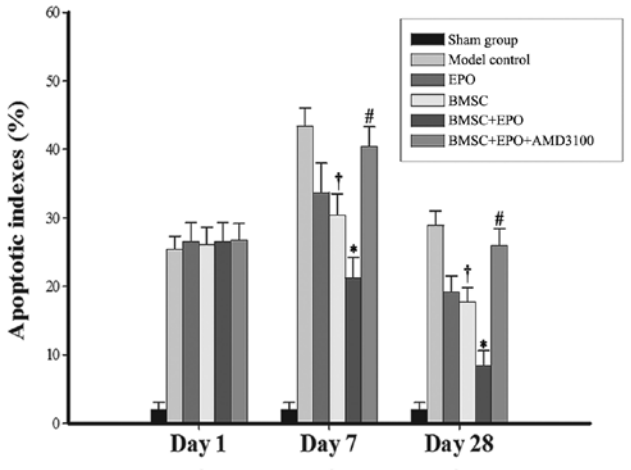

Figure 7. Apoptotic indexes at different time points in each group. *P<0.05 vs. the sham-operated (sham) group, model control, EPO, BMSC and BMSC + EPO + AMD3100 groups; †P<0.05 vs. the model control; #P>0.05 vs. the model control. The data are plotted as the means ± SD. EPO, erythropoietin; BMSC, bone marrow-derived mesenchymal stem cell.

EPO has attracted widespread attention is not only due to its primary role in erythropoiesis, but also due to its effects on the non-hematopoietic system, such as neurotrophic and neuroprotective effects, and its regulatory role in embryonic development (40). Over the past two decades, a series of basic and clinical studies have been carried out worldwide and it has been confirmed that EPO exerts neuroprotective effects in acute SCI (41,42). Gorio *et al* (26) produced a model of acute thoracic spinal cord contusion with an aneurysm clip, after which immediate intraperitoneal injections of EPO were administered. Compared with the control group, inflammation in the experimental group was significantly inhibited, void formation in the spinal cord was apparently reduced and motor function was significantly improved (26). Celik *et al* (43) created a spinal cord ischemia reperfusion model using an abdominal aortic clamp, and rhEPO was administered 48 h after modeling. The functional neurological status in the rhEPO group was better compared with that of the control group, and the apoptosis of motor neurons in the rhEPO group was significantly reduced compared with the control group (43). In addition to the effects described above, EPO is a stem cell mobilization agent, which mobilizes hematopoietic stem cells and BMSCs to participate in the repair of a variety of tissues and organs (30,31). In the present study, we provide evidence that EPO is able to mobilize BMSCs to migrate to the lesion site following SCI and enhance their neuroprotective effects.

The SDF-1/CXCR4 axis is of crucial importance in the migration of BMSCs to the lesion sites, as it has been demonstrated that the recruitment of BMSCs is terminated when the SDF-1/CXCR4 axis is impaired (14-17,44). Hence, the increased secretion of SDF-1 at the lesion site promotes the homing of circulating CXCR4-positive cells. BMSCs stimulated with SDF-1 express multiple genes, 11 of which regulate cell migration (45). In a previous study, GFP-labeled BMSCs were grafted into rats with unilateral mandibular distraction osteogenesis and SDF-1 was found to promote the migration of BMSCs *in vivo* and *in vitro*, and this effect was inhibited by AMD3100, a CXCR4-blocking antibody (46). It has been demonstrated that CXCR4 mediates the migration of BMSCs to ischemic kidneys and this CXCR4-mediated migration of BMSCs was inhibited by the CXCR4 antagonist, AMD3100 (47). Moreover, the transplantation of BMSCs to the burn wound area in an animal model promoted the epithelialization of the wound; however, preconditioning with AMD3100 significantly inhibited the

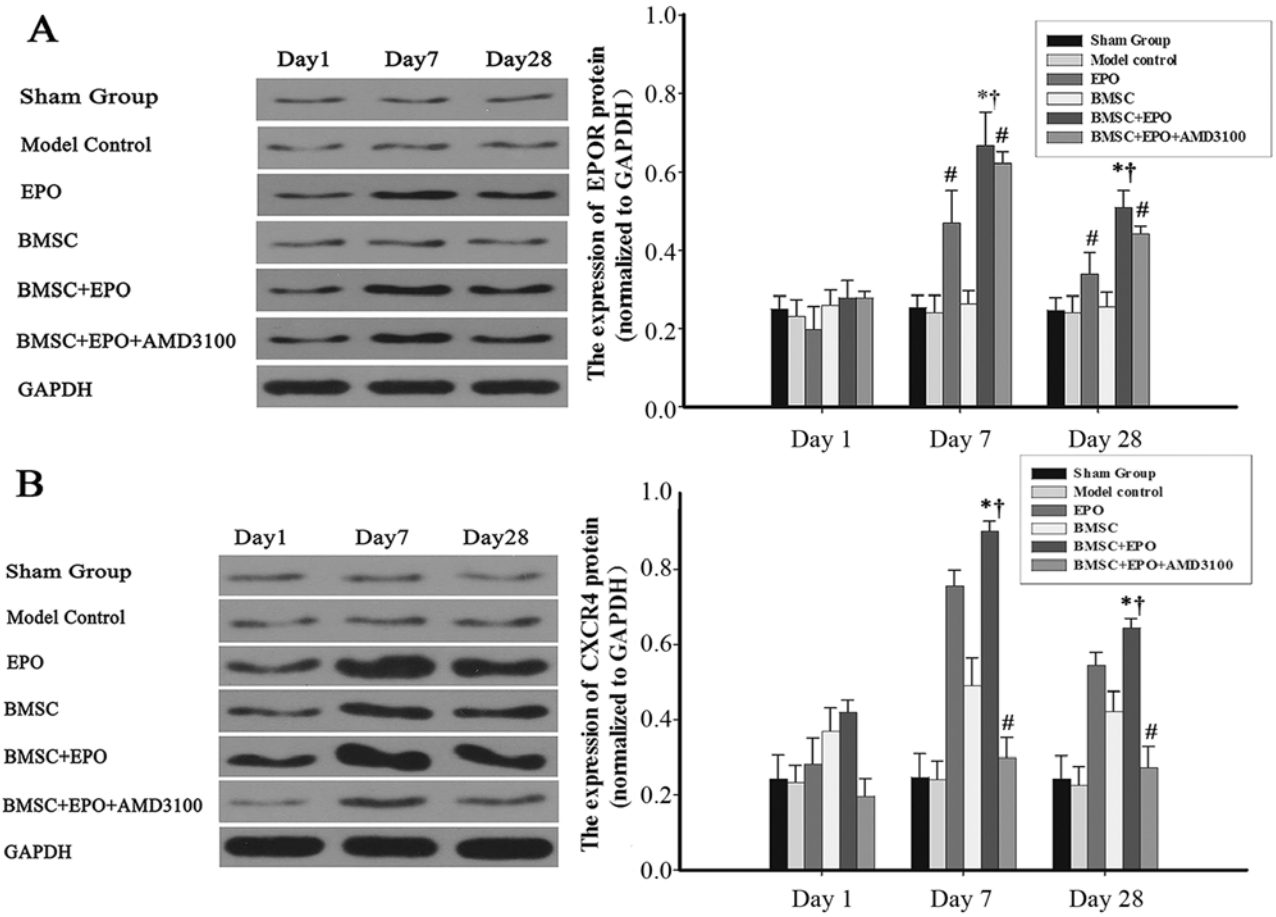

Figure 8. Evaluation of (A) EPOR and (B) CXCR4 protein expression on days 1, 7 and 28 post-operation in each group by western blot analysis. The relative protein abundance was determined following normalization to GAPDH. *P<0.05 vs. the sham-operated (sham) group and model control; †P<0.05 vs. the EPO, BMSC and BMSC + EPO + AMD3100 groups; #P<0.05 vs. the model control. The data are plotted as the means ± SD. EPO, erythropoietin; BMSC, bone mesenchymal stem cell; CXCR4, CXC chemokine receptor 4; EPOR, erythropoietin receptor.

mobilization of the BMSCs to the wound area (48). In another study on SCI, BMSCs were administered by lumbar intrathecal injection 2 days after modeling, and the results indicated that the SDF-1/CXCR4 axis participated in the migration of BMSCs into the injured zone (49). Taken together, these findings confirm that the association between locally generated SDF-1 and its ligand CXCR4, expressed on the surface of BMSCs, plays a crucial role in the homing of transplanted cells. This was consistent with the findings of our study; we demonstrated that EPO significantly upregulated the protein expression of CXCR4 in the spinal cord samples and promoted the migration of BMSCs, whereas these effects were markedly inhibited when the BMSCs were co-transplanted with AMD3100.

There is evidence to confirm the involvement of chemokines as migratory starting points in the trafficking of BMSCs to the lesion site (50). Modulating the detrimental environment can facilitate the recruitment of BMSCs into the target region. The injured tissue undergoes acute or chronic immunological responses, and BMSCs migrating to these regions will come into contact with various immunocytes in the local area. TNF-α has previously been demonstrated to play a role in the upregulation of matrix metalloproteinases (MMPs) in BMSCs, which strongly stimulates the chemotactic migration of the cells through the extracellular matrix (51). In a previous study, it was confirmed that systemically transplanted regulatory T cells or locally administered aspirin significantly enhanced the survival of BMSCs and promoted bone regeneration through the inhibition of interferon-γ (IFN-γ) and TNF-α in injured bone tissues (52). Another previous study demonstrated that EPO inhibited the production of TNF by glial cells, which were exposed to trimethyltin, an apoptosis-inducing toxin (53). In accordance with these findings, in this study, we found that EPO significantly decreased thye levels of TNF-α and increased the levels of SDF-1 in the injured spinal cord, and these effects were attenuated by AMD3100.

Another possible mechanism is that EPO inhibits the cell apoptosis (54). Apoptosis is a significant element of the delayed secondary damage which occurs following SCI. EPO has been documented to play a significant role in preventing the apoptosis of neurons in a rat model of nerve root crush injury (54). EPO has also been shown to prevent spinal cord cell apoptosis following acute traumatic injury in rats (55). Following transient spinal cord ischemia, almost no apoptotic pattern was detectable (no TUNEL labeling present) in EPO treated ventral horn motor neurons (56), while in a model of crush injury of the spinal nerve root, EPO prevented apoptosis in dorsal root ganglion neurons (54). In this study, we detected the AI in the injured spinal cords by the TUNEL assay. The

number of apoptotic cells in the spinal cords significantly increased following SCI. The number of apoptotic cells significantly decreased in the BMSC + EPO group compared with the model control and BMSC groups, and this effect was attenuated by AMD3100. This result indicated that EPO enhanced the anti-apoptotic effect of the BMSCs by acting on the SDF-1/CXCR4 axis.

In the present study, two complementary behavioural tests were adopted to evaluate and accurately estimate the recovery of locomotor functions following SCI: the BBB Locomotor Rating Scale and the grid walk test. In both tests, the animals in the model control group showed spontaneous recovery following SCI, which was interpreted by the pattern of the injury. Rats in the BMSC + EPO and BMSC groups showed a more significant improvement in the recovery of locomotor functions compared with the model control group. Significant improvements in locomotor function were also observed in the BMSC + EPO group compared with the BMSC group, while no significant difference was observed between the model control and BMSC + EPO + AMD3100 group. These outcomes demonstrated that the administration of EPO, in conjunction with BMSCs, enhances the neurological recovery of rats with SCI by acting on the SDF-1/CXCR4 axis.

In conclusion, the findings of the present study confirm that EPO mobilizes BMSCs to the lesion site following SCI and enhances the anti-apoptotic effects of BMSCs by upregulating the expression of the SDF-1/CXCR4 axis. EPO enhances the therapeutic benefits of BMSCs and improves neurological outcomes following SCI. Thus, the combined strategy of BMSC transplantation with EPO therapy exhibits potential for the treatment of traumatic SCI.

Acknowledgements

The authors appreciate the assistance provided by Chen Shen and Yu Lin (Renmin Hospital of Wuhan University, Wuhan, China) during the processing of this manuscript. This study was financially supported by the Project of the Natural Science Foundation of Hubei, China (grant no. 2013CFC035).

References

1. Martinez AM, Goulart CO, Ramalho BS, Oliveira JT and Almeida FM: Neurotrauma and mesenchymal stem cells treatment: From experimental studies to clinical trials. World J Stem Cells 6: 179-194, 2014.
2. Varma AK, Das A, Wallace G IV, Barry J, Vertegel AA, Ray SK and Banik NL: Spinal cord injury: a review of current therapy, future treatments, and basic science frontiers. Neurochem Res 38: 895-905, 2013.
3. Bracken MB: Steroids for acute spinal cord injury. Cochrane Database Syst Rev 1: CD001046, 2012.
4. Vawda R and Fehlings MG: Mesenchymal cells in the treatment of spinal cord injury: current and future perspectives. Curr Stem Cell Res Ther 8: 25-38, 2013.
5. Mothe AJ and Tator CH: Advances in stem cell therapy for spinal cord injury. J Clin Invest 122: 3824-3834, 2012.
6. Himes BT, Neuhuber B, Coleman C, Kushner R, Swanger SA, Kopen GC, Wagner J, Shumsky JS and Fischer I: Recovery of function following grafting of human bone marrow-derived stromal cells into the injured spinal cord. Neurorehabil Neural Repair 20: 278-296, 2006.
7. Neuhuber B, Timothy Himes B, Shumsky JS, Gallo G and Fischer I: Axon growth and recovery of function supported by human bone marrow stromal cells in the injured spinal cord exhibit donor variations. Brain Res 1035: 73-85, 2005.
8. Abrams MB, Dominguez C, Pernold K, Reger R, Wiesenfeld-Hallin Z, Olson L and Prockop D: Multipotent mesenchymal stromal cells attenuate chronic inflammation and injury-induced sensitivity to mechanical stimuli in experimental spinal cord injury. Restor Neurol Neurosci 27: 307-321, 2009.
9. Novikova LN, Brohlin M, Kingham PJ, Novikov LN and Wiberg M: Neuroprotective and growth-promoting effects of bone marrow stromal cells after cervical spinal cord injury in adult rats. Cytotherapy 13: 873-887, 2011.
10. Stolzing A and Scutt A: Effect of reduced culture temperature on antioxidant defences of mesenchymal stem cells. Free Radic Biol Med 41: 326-338, 2006.
11. Hoffmann J, Glassford AJ, Doyle TC, Robbins RC, Schrepfer S and Pelletier MP: Angiogenic effects despite limited cell survival of bone marrow-derived mesenchymal stem cells under ischemia. Thorac Cardiovasc Surg 58: 136-142, 2010.
12. Yi T and Song SU: Immunomodulatory properties of mesenchymal stem cells and their therapeutic applications. Arch Pharm Res 35: 213-221, 2012.
13. Galipeau J: The mesenchymal stromal cells dilemma - does a negative phase III trial of random donor mesenchymal stromal cells in steroid-resistant graft-versus-host disease represent a death knell or a bump in the road? Cytotherapy 15: 2-8, 2013.
14. Cencioni C, Capogrossi MC and Napolitano M: The SDF-1/CXCR4 axis in stem cell preconditioning. Cardiovasc Res 94: 400-407, 2012.
15. Liu X, Duan B, Cheng Z, Jia X, Mao L, Fu H, Che Y, Ou L, Liu L and Kong D: SDF-1/CXCR4 axis modulates bone marrow mesenchymal stem cell apoptosis, migration and cytokine secretion. Protein Cell 2: 845-854, 2011.
16. Gong J, Meng HB, Hua J, Song ZS, He ZG, Zhou B and Qian MP: The SDF-1/CXCR4 axis regulates migration of transplanted bone marrow mesenchymal stem cells towards the pancreas in rats with acute pancreatitis. Mol Med Rep 9: 1575-1582, 2014.
17. Ghadge SK, Mühlstedt S, Ozcelik C and Bader M: SDF-1α as a therapeutic stem cell homing factor in myocardial infarction. Pharmacol Ther 129: 97-108, 2011.
18. Yu J, Li M, Qu Z, Yan D, Li D and Ruan Q: SDF-1/CXCR4-mediated migration of transplanted bone marrow stromal cells toward areas of heart myocardial infarction through activation of PI3K/Akt. J Cardiovasc Pharmacol 55: 496-505, 2010.
19. Wang Y, Deng Y and Zhou GQ: SDF-1α/CXCR4-mediated migration of systemically transplanted bone marrow stromal cells towards ischemic brain lesion in a rat model. Brain Res 1195: 104-112, 2008.
20. Koury MJ and Bondurant MC: Maintenance by erythropoietin of viability and maturation of murine erythroid precursor cells. J Cell Physiol 137: 65-74, 1988.
21. Rölfing JH, Jensen J, Jensen JN, Greve AS, Lysdahl H, Chen M, Rejnmark L and Bünger C: A single topical dose of erythropoietin applied on a collagen carrier enhances calvarial bone healing in pigs. Acta Orthop 85: 201-209, 2014.
22. Teixeira M, Rodrigues-Santos P, Garrido P, Costa E, Parada B, Sereno J, Alves R, Belo L, Teixeira F, Santos-Silva A and Reis F: Cardiac antiapoptotic and proproliferative effect of recombinant human erythropoietin in a moderate stage of chronic renal failure in the rat. J Pharm Bioallied Sci 4: 76-83, 2012.
23. Weng S, Zhu X, Jin Y, Wang T and Huang H: Protective effect of erythropoietin on myocardial infarction in rats by inhibition of caspase-12 expression. Exp Ther Med 2: 833-836, 2011.
24. Chen S, Li J, Peng H, Zhou J and Fang H: Administration of erythropoietin exerts protective effects against glucocorticoid-induced osteonecrosis of the femoral head in rats. Int J Mol Med 33: 840-848, 2014.
25. Xiong M, Chen S, Yu H, Liu Z, Zeng Y and Li F: Neuroprotection of erythropoietin and methylprednisolone against spinal cord ischemia-reperfusion injury. J Huazhong Univ Sci Technolog Med Sci 31: 652-656, 2011.
26. Gorio A, Gokmen N, Erbayraktar S, Yilmaz O, Madaschi L, Cichetti C, Di Giulio AM, Vardar E, Cerami A and Brines M: Recombinant human erythropoietin counteracts secondary injury and markedly enhances neurological recovery from experimental spinal cord trauma. Proc Natl Acad Sci USA 99: 9450-9455, 2002.
27. Choi D, Schroer SA, Lu SY, Wang L, Wu X, Liu Y, Zhang Y, Gaisano HY, Wagner KU, Wu H, *et al*: Erythropoietin protects against diabetes through direct effects on pancreatic beta cells. J Exp Med 207: 2831-2842, 2010.
28. MacRedmond R, Singhera GK and Dorscheid DR: Erythropoietin inhibits respiratory epithelial cell apoptosis in a model of acute lung injury. Eur Respir J 33: 1403-1414, 2009.

29. Kakavas S, Demestiha T, Vasileiou P and Xanthos T: Erythropoetin as a novel agent with pleiotropic effects against acute lung injury. Eur J Clin Pharmacol 67: 1-9, 2011.
30. Zwezdaryk KJ, Coffelt SB, Figueroa YG, Liu J, Phinney DG, LaMarca HL, Florez L, Morris CB, Hoyle GW and Scandurro AB: Erythropoietin, a hypoxia-regulated factor, elicits a pro-angiogenic program in human mesenchymal stem cells. Exp Hematol 35: 640-652, 2007.
31. Liu NM, Tian J, Wang WW, Han GF, Cheng J, Huang J and Zhang JY: Effect of erythropoietin on mesenchymal stem cell differentiation and secretion in vitro in an acute kidney injury microenvironment. Genet Mol Res 12: 6477-6487, 2013.
32. Nair AM, Tsai YT, Shah KM, Shen J, Weng H, Zhou J, Sun X, Saxena R, Borrelli J Jr and Tang L: The effect of erythropoietin on autologous stem cell-mediated bone regeneration. Biomaterials 34: 7364-7371, 2013.
33. Kwon BK, Oxland TR and Tetzlaff W: Animal models used in spinal cord regeneration research. Spine 27: 1504-1510, 2002.
34. Deng W, Bivalacqua TJ, Chattergoon NN, Jeter JR Jr and Kadowitz PJ: Engineering ex vivo-expanded marrow stromal cells to secrete calcitonin gene-related peptide using adenoviral vector. Stem Cells 22: 1279-1291, 2004.
35. Bobadilla M, Sainz N, Abizanda G, Orbe J, Rodriguez JA, Páramo JA, Prósper F and Pérez-Ruiz A: The CXCR4/SDF1 axis improves muscle regeneration through MMP-10 activity. Stem Cells Dev 23: 1417-1427, 2014.
36. Basso DM, Beattie MS and Bresnahan JC: A sensitive and reliable locomotor rating scale for open field testing in rats. J Neurotrauma 12: 1-21, 1995.
37. Wang S, Wu Z, Chiang P, Fink DJ and Mata M: Vector-mediated expression of erythropoietin improves functional outcome after cervical spinal cord contusion injury. Gene Ther 19: 907-914, 2012.
38. McDonald JW and Sadowsky C: Spinal-cord injury. Lancet 359: 417-425, 2002.
39. Noguchi CT, Wang L, Rogers HM, Teng R and Jia Y: Survival and proliferative roles of erythropoietin beyond the erythroid lineage. Expert Rev Mol Med 10: e36, 2008.
40. Paschos N, Lykissas MG and Beris AE: The role of erythropoietin as an inhibitor of tissue ischemia. Int J Biol Sci 4: 161-168, 2008.
41. Grasso G, Sfacteria A, Passalacqua M, Morabito A, Buemi M, Macrì B, Brines ML and Tomasello F: Erythropoietin and erythropoietin receptor expression after experimental spinal cord injury encourages therapy by exogenous erythropoietin. Neurosurgery 56: 821-827, discussion 821-827, 2005.
42. Qi C, Xu M, Gan J, Yang X, Wu N, Song L, Yuan W and Liu Z: Erythropoietin improves neurobehavior by reducing dopaminergic neuron loss in a 6 hydroxydopamine induced rat model. Int J Mol Med 34: 440-450, 2014.
43. Celik M, Gökmen N, Erbayraktar S, Akhisaroglu M, Konakc S, Ulukus C, Genc S, Genc K, Sagiroglu E, Cerami A and Brines M: Erythropoietin prevents motor neuron apoptosis and neurologic disability in experimental spinal cord ischemic injury. Proc Natl Acad Sci USA 99: 2258-2263, 2002.
44. Kitaori T, Ito H, Schwarz EM, Tsutsumi R, Yoshitomi H, Oishi S, Nakano M, Fujii N, Nagasawa T and Nakamura T: Stromal cell-derived factor 1/CXCR4 signaling is critical for the recruitment of mesenchymal stem cells to the fracture site during skeletal repair in a mouse model. Arthritis Rheum 60: 813-823, 2009.
45. Stich S, Haag M, Häupl T, Sezer O, Notter M, Kaps C, Sittinger M and Ringe J: Gene expression profiling of human mesenchymal stem cells chemotactically induced with CXCL12. Cell Tissue Res 336: 225-236, 2009.
46. Jaerve A, Schira J and Müller HW: Concise review: the potential of stromal cell-derived factor 1 and its receptors to promote stem cell functions in spinal cord repair. Stem Cells Transl Med 1: 732-739, 2012.
47. Liu N, Patzak A and Zhang J: CXCR4-overexpressing bone marrow-derived mesenchymal stem cells improve repair of acute kidney injury. Am J Physiol Renal Physiol 305: F1064-F1073, 2013.
48. Hu C, Yong X, Li C, Lü M, Liu D, Chen L, Hu J, Teng M, Zhang D, Fan Y and Liang G: CXCL12/CXCR4 axis promotes mesenchymal stem cell mobilization to burn wounds and contributes to wound repair. J Surg Res 183: 427-434, 2013.
49. Fan DY, Liu Y, Xu FC, *et al*: CXCL12/CXCR4 biology axis effects on the repair of spinal cord injury with bone marrow mesenchymal stem cells. J Clin Rehabil Tissue Eng Res 15: 6651-6656, 2011.
50. Karp JM and Leng Teo GS: Mesenchymal stem cell homing: the devil is in the details. Cell Stem Cell 4: 206-216, 2009.
51. Ries C, Egea V, Karow M, Kolb H, Jochum M and Neth P: MMP-2, MT1-MMP, and TIMP-2 are essential for the invasive capacity of human mesenchymal stem cells: differential regulation by inflammatory cytokines. Blood 109: 4055-4063, 2007.
52. Liu Y, Wang L, Kikuiri T, Akiyama K, Chen C, Xu X, Yang R, Chen W, Wang S and Shi S: Mesenchymal stem cell-based tissue regeneration is governed by recipient T lymphocytes via IFN-γ and TNF-α. Nat Med 17: 1594-1601, 2011.
53. Villa P, Bigini P, Mennini T, Agnello D, Laragione T, Cagnotto A, Viviani B, Marinovich M, Cerami A, Coleman TR, *et al*: Erythropoietin selectively attenuates cytokine production and inflammation in cerebral ischemia by targeting neuronal apoptosis. J Exp Med 198: 971-975, 2003.
54. Sekiguchi Y, Kikuchi S, Myers RR and Campana WM: ISSLS prize winner: Erythropoietin inhibits spinal neuronal apoptosis and pain following nerve root crush. Spine 28: 2577-2584, 2003.
55. Arishima Y, Setoguchi T, Yamaura I, Yone K and Komiya S: Preventive effect of erythropoietin on spinal cord cell apoptosis following acute traumatic injury in rats. Spine 31: 2432-2438, 2006.
56. Knabe W, Sirén AL, Ehrenreich H and Kuhn HJ: Expression patterns of erythropoietin and its receptor in the developing spinal cord and dorsal root ganglia. Anat Embryol (Berl) 210: 209-219, 2005.